JOURNAL OF COMPUTATIONAL PHYSICS 56, 51–64 (1984)

Smoothing and Spatial Grid Effects in Implicit Particle Simulation*

BRUCE I. COHEN, A. BRUCE LANGDON, AND ALEX FRIEDMAN

Lawrence Livermore National Laboratory, University of California, Livermore, California 94550

Received September 15, 1983

Convergence and linear dispersion properties in implicit particle codes used in plasma simulation are investigated. Inconsistent spatial smoothing and simplified spatial differencing are shown to be closely related and degrade convergence and, if suitable care is not taken, stability. The convergence and dispersion properties of non-iterated, partially converged solution schemes are calculated. A careful combination of an implicit field solution with extrapolation of particle quantities using a previously calculated electric field need not degrade linear stability and dispersion characteristics. Even with some degradation of convergence, and with only one pass through the coupled particle and field equations on each time step, code performance can be entirely satisfactory if good stability and dispersion characteristics are preserved.

1. INTRODUCTION

The recently developed direct implicit particle simulation method [1, 2] relaxes severe stability constraints on time step that exist in explicit formulations, e.g., $\omega_p \Delta t < 0(1)$, where ω_p is the plasma frequency. This permits more efficient simulation of long time-scale phenomena at long wavelengths. Much less stringent residual time-step constraints arise having to do with accuracy of the particle orbits and of the plasma dielectric response [3]. The direct implicit method readily extends to a two-dimensional magnetized algorithm [4] and to an electromagnetic version [5].

A number of important aspects of the direct implicit particle simulation method have been studied theoretically in [2] and [3]. One-dimensional simulations with the direct method have been reported in [1, 4, 6]. Barnes and co-workers have performed

0021-9991/84 $3.00

two-dimensional electrostatic simulations with an applied magnetic field [4]. Denavit is using a direct method in a hybrid simulation model [7]. Menyuk has applied these ideas to solve discrete mapping equations for Hamiltonian systems more efficiently [8].

In order to achieve a practical advantage with implicit particle simulation over conventional explicit methods, stability at large $\omega_p \Delta t$ must be preserved when the effects of a spatial mesh and spatial smoothing are included. In addition, when shortcuts are taken in the spatial differencing with the aim of reducing the size of the matrix field equation and what must be collected and stored from particles [2], convergence and linear dispersion properties must be re-examined. Such considerations are of great importance in improving the economy and quality of two- and three-dimensional simulations. Furthermore, nonlinear accuracy may be improved by combining extrapolation using previously calculated quantities with an implicit solution of the implicit field-particle equations.

In [2] and [3] we investigated, among other things, dispersion characteristics of time-integration schemes ignoring spatial differencing in [3] and considered some spatial differencing issues in [2]. In [2] we found that rigorous adherence to systematic and rigorous differencing and interpolation procedures ("strict" differencing) led to good convergence and stability characteristics, but that ad hoc spatial differencing and inconsistent spatial smoothing could degrade convergence and stability. We extend that discussion here and demonstrate that convergence and linear dispersion characteristics are related. Use of the electric field from the last previous time step as a first guess for the field at the advanced time level improves accuracy and does *not* influence linear dispersion and stability if strict spatial differencing and consistent smoothing are used. With simplified differencing or inconsistent smoothing, extrapolation with an old electric-field value can introduce a phase error that degrades linear dispersion properties. An improved extrapolation scheme is presented that does not introduce phase errors. The analysis given in this paper is one dimensional; the extension to two dimensions is straightforward, as demonstrated in [2].

The plan of the paper is as follows. Section 2 reviews the rudiments of the direct implicit particle simulation method. In Section 3 we elaborate on the discussion of the convergence of the field-particle equations that appeared in [2]. This provides a prologue to Section 4 in which we derive the cold-plasma linear dispersion relation for several versions of the direct implicit particle simulation method. The analysis determines the influences of spatial differencing, smoothing, and electric-field extrapolation. We find that the theory agrees favorably with one-dimensional simulation examples. We present conclusions in Section 5.

2. The Direct Implicit Method

The essence of the direct implicit method is illustrated in the following one-dimensional electrostatic example. The charge density is

$$\rho_j^{n+1} = q \sum_k S(X_j - x_k^{n+1}), \tag{1}$$

where j is the grid index, k is the particle index, q is the charge, S is the particle-grid interpolation spline, and the superscript $n+1$ denotes the time level. If we expand S with respect to a predicted position $\tilde{x}_k^{n+1}$ using known positions, velocities, and accelerations (see Section 4.1), then

$$S(X_j - x_k^{n+1}) \simeq S(X_j - \tilde{x}_k^{n+1}) + (x_k^{n+1} - \tilde{x}_k^{n+1})\,(d/d\tilde{x}_k)\,S(X_j - \tilde{x}_k^{n+1}). \tag{2}$$

The particle equation of motion can be written as

$$x_k^{n+1} = \beta\,\Delta t^2\, a_k^{n+1} + \tilde{x}_k^{n+1} = \beta(q/m)\,\Delta t^2\,\Delta x \sum_i S(X_i - \tilde{x}_k^{n+1})\,E_i^{n+1} + \tilde{x}_k^{n+1}, \tag{3}$$

where β is a parameter controlling implicitness. With summation over species understood, Poisson's equation in rationalized c.g.s. units becomes

$$-\frac{\phi_{j+1}^{n+1} - 2\phi_j^{n+1} + \phi_{j-1}^{n+1}}{\Delta x^2}$$

$$+\beta\frac{q^2\,\Delta t^2\,\Delta x}{m}\sum_{k,i} S(X_i - \tilde{x}_k^{n+1})\frac{d}{d\tilde{x}_k}S(X_j - \tilde{x}_k^{n+1})\frac{\phi_{i+1}^{n+1} - \phi_{i-1}^{n+1}}{2\,\Delta x} = \tilde{\rho}_j^{n+1}, \tag{4}$$

where $\tilde{\rho}_j^{n+1}$ is the charge density based on use of $\tilde{x}_k^{n+1}$ in Eq. (1). For linear splines there is no contribution to Eq. (4) for $|i-j| > 1$, $\Delta x^2\, dS/d\tilde{x}_k = \pm 1$ or 0, and the field equation is penta-diagonal. The relative error in the expansion procedure is $\beta\omega_{tr}^2\,\Delta t^2 = |\beta qE\,\Delta t^2/mL_E|$, where ω_{tr} is the electrostatic trapping frequency and L_E is the length scale over which the electric field E varies. Further discussion of this form of the direct method is found in [1] and Section 2 of [2]. Appendix A of [2] demonstrates the connection of the implicit moment and direct implicit methods.

3. Convergence

In [2], Poisson's equation was cast in an iterative form,

$$-\nabla\cdot[(1+\chi^{(r)})\nabla\,\delta\phi^{(r+1)}] = \rho^{(r)} + \nabla^2\phi^{(r)}, \tag{5}$$

where $\chi^{(r)}$ is the effective susceptibility deducible from the second term in Eq. (4), the superscript (r) or $(r+1)$ indicates an iteration level, and the time level $n+1$ is

understood. The ratio of successive residuals $|\rho^{(r+1)} - \nabla \cdot \mathbf{E}^{(r+1)}|$ is a measure of the convergence of this iteration. With only one pass through the particle and field equations on each time step, as is the case with all applications of the direct method so far [1, 4, 6], the residual $|\rho^{(1)} - \nabla \cdot \mathbf{E}^{(1)}|$ gives a quantitative measure of the accuracy and convergence of the solutions of the coupled particle and field equations.

On each iteration the particle position in a one-dimensional formulation is updated according to

$$x_{n+1}^{(r+1)} = \beta \, \Delta t^2 \, a_{n+1}^{(r+1)}(x_{n+1}^{(r+1)}) + \tilde{x}_{n+1}, \tag{6}$$

which is an iterative refinement of Eq. (3) and was described in detail in Section 3.1 of [2]. The increment $\delta x_k^{(r+1)} \equiv x_k^{(r+1)} - x_k^{(r)}$ is given by

$$\delta x_k^{(r+1)} = \beta q \, \Delta t^2 \, m^{-1} \, \Delta x \sum_j S(X_j - x_k^{(r)}) \, \delta E_j^{(r+1)} \times \left[1 - \beta q \, \Delta t^2 \, m^{-1} \, \Delta x \sum_i E_i \frac{\partial}{\partial x_k} S(X_i - x_k^{(r)}) \right]^{-1} \tag{7}$$

through linear order. From δx we form $\delta \rho^{(r+1)} = -\nabla \cdot [\rho^{(r)} \, \delta \mathbf{x}^{(r+1)}] = -\nabla \cdot [\chi^{(r)} \, \delta \mathbf{E}^{(r+1)}]$, where

$$\chi_{j+1/2,j'}^{(r)} = \sum_{k \in j+1/2} \beta N^{-1} \, \Delta t^2 \, q^2 m^{-1} S(X_{j'} - x_k^{(r)}) \tag{8a}$$

and

$$N \equiv 1 - \beta q \, \Delta t^2 \, m^{-1} \, \Delta x \sum_i E_i \frac{\partial}{\partial x_k} S(X_i - x_k^{(r)}). \tag{8b}$$

Hence, by construction

$$\begin{aligned} |\rho^{(r+1)} - \nabla \cdot \mathbf{E}^{(r+1)}| &= |\rho^{(r)} + \delta \rho^{(r+1)} - \nabla \cdot \mathbf{E}^{(r)} - \nabla \cdot \delta \mathbf{E}^{(r+1)}| \\ &= |\nabla \cdot (1 + \chi^{(r)}) \, \delta \mathbf{E}^{(r+1)} + \delta \rho^{(r+1)} - \nabla \cdot \delta \mathbf{E}^{(r+1)}| \\ &= |\nabla \cdot \chi^{(r)} \, \delta \mathbf{E}^{(r+1)} + \delta \rho^{(r+1)}| = 0, \end{aligned} \tag{9}$$

through order $\beta \omega_{tr}^2 \, \Delta t^2$.

If we omit the Newton–Raphson correction in Eq. (8a) by setting $N \equiv 1$, as has been done in all applications, convergence is weaker,

$$\frac{|\rho^{(r+1)} - \nabla \cdot \mathbf{E}^{(r+1)}|}{|\rho^{(r)} - \nabla \cdot \mathbf{E}^{(r)}|} = \frac{|\nabla \cdot (\chi^{(r)} \beta q m^{-1} \, \Delta t^2 \, \partial E^{(r)} / \partial x) \, \delta \mathbf{E}^{(r+1)}|}{|\nabla \cdot (1 + \chi^{(r)}) \, \delta \mathbf{E}^{(r+1)}|}, \tag{10}$$

because the numerator no longer vanishes at this order.

With consistent spatial filtering [2], Poisson's equation is

$$-\nabla \cdot [1 + S_2 S_1 \chi^{(r)}] \nabla \delta\phi_s^{(r+1)} = \rho_s^{(r)} + \nabla^2 \phi_s^{(r)}, \tag{11}$$

where S_1 and S_2 are smoothing operators acting on everything to their right, and $\rho_s \equiv S_2 S_1 \rho$ and $(\phi_s, \delta\phi_s) \equiv S_2(\phi, \delta\phi)$ are the smoothed charge density and potentials. Weaker convergence also results when inconsistent smoothing is used. For example, if $\chi^{(r)}$ were inconsistently smoothed so that $\nabla \cdot [\chi^{(r)}\, \delta\mathbf{E}^{(r+1)}] \to \nabla \cdot [\tilde{S}_2 \tilde{S}_1 \chi^{(r)}\, \delta\mathbf{E}^{(r+1)}]$, then

$$\frac{|\rho^{(r+1)} - \nabla \cdot \mathbf{E}^{(r+1)}|}{|\rho^{(r)} - \nabla \cdot \mathbf{E}^{(r)}|} = \frac{|\nabla \cdot (\tilde{S}_2 \tilde{S}_1 - S_2 S_1)\chi^{(r)}\, \delta\mathbf{E}^{(r+1)}|}{|\nabla \cdot (1 + \chi^{(r)})\, \delta\mathbf{E}^{(r+1)}|}. \tag{12}$$

For typical smoothing operators, convergence will be worse for densities and electric fields that vary rapidly in space. Barnes *et al.* [4] have found much more reliable code behavior with use of consistent spatial smoothing, while inconsistent smoothing led to grief.

Simplified, ad hoc differencing schemes [2, 4] have been employed to reduce the bandwidth of the matrix field equation, a matter of great importance in two- and three-dimensional applications. However, simplified differencing can degrade convergence. Two types of errors can arise that contribute to $|\rho^{(r+1)} - \nabla \cdot \mathbf{E}^{(r+1)}|$. The first has been encountered already and results from the inconsistency of $\chi^{(r)}$ and the equations leading to $\delta\mathbf{x}^{(r+1)}$ and $\rho^{(r+1)}$. The other error is due to the representation of $\nabla \cdot \chi\, \delta\mathbf{E}$ and is much like that due to inconsistent spatial smoothing. A representative calculation gives

$$\frac{|\rho^{(r+1)} - \nabla \cdot \mathbf{E}^{(r+1)}|}{|\rho^{(r)} - \nabla \cdot \mathbf{E}^{(r)}|} = \frac{|(\nabla \cdot \chi^{(r)}\, \delta\mathbf{E}^{(r+1)})' - \nabla \cdot \chi^{(r)}\, \delta\mathbf{E}^{(r+1)}|}{|\nabla \cdot (1 + \chi^{(r)})\, \delta\mathbf{E}^{(r+1)}|}, \tag{13}$$

where $\nabla \cdot \chi\, \delta\mathbf{E}$ is a form using strict differencing, and $(\,)'$ indicates the simplified-differencing version. The derivation of Eq. (13) is the same as Eq. (12); we have added and subtracted the strictly differenced $\nabla \cdot [\chi^{(r)}\, \delta\mathbf{E}^{(r+1)}]$ to the field equation, using the fact that the numerator of Eq. (13) vanishes for strict differencing. Rapid variations in the plasma density lead to a loss of convergence through the difference in susceptibilities. Spatial smoothing may help here. However, even in a uniform plasma, different electric-field stencils can cause a loss of convergence at short wavelengths.

4. Linear Dispersion Relation

4.1. *Grid Effects*

Analysis of the dispersion relation for a simple harmonic oscillator [3] gives useful information on stability at large $\omega\, \Delta t$ and accuracy at small $\omega\, \Delta t$. Consider iteration schemes as described in [2] and suggested here in Eq. (5) with the initial estimate

$a_{n+1}^{(0)} = 0$ and strict spatial differencing. A *linear* expansion of the equations of motion for a small-amplitude oscillation demonstrates that all linear quantities converge exactly on the initial iteration step. Thus, analysis of just the implicit predictor step is sufficient and is appropriate to all of the applications of the direct implicit method [1, 4, 6].

We consider here two general classes of time integration schemes described in [3]. The class "C" schemes introduced in [9] and analyzed in [3] are represented by the difference equations

$$\mathbf{x}_{n+1} = \mathbf{x}_n + \mathbf{v}_{n+1/2}\,\Delta t + c_0(\mathbf{a}_{n+1} - \mathbf{a}_n)\,\Delta t^2 + c_1(\mathbf{a}_n - \mathbf{a}_{n-1})\,\Delta t^2 + \cdots$$
$$\mathbf{v}_{n+1/2} = \mathbf{v}_{n-1/2} + \mathbf{a}_n\,\Delta t.$$

In these schemes, $\tilde{\mathbf{x}}_{n+1} = \mathbf{x}_n + \mathbf{v}_{n+1/2}\,\Delta t - c_0\mathbf{a}_n\,\Delta t + c_1(\mathbf{a}_n - \mathbf{a}_{n-1})\,\Delta t^2 + \cdots$. The class "$D_1$" scheme introduced in [3] can be represented in the form

$$\mathbf{x}_{n+1} = \mathbf{x}_n + \mathbf{v}_{n+1/2}\,\Delta t$$
$$\mathbf{v}_{n+1/2} = \mathbf{v}_{n-1/2} + \bar{\mathbf{a}}_n\,\Delta t,$$

where $\bar{\mathbf{a}}_n = 1/2(\bar{\mathbf{a}}_{n-1} + \mathbf{a}_{n+1})$. Here $\tilde{\mathbf{x}}_{n+1} = \mathbf{x}_n + \mathbf{v}_{n-1/2}\,\Delta t + 1/2\bar{\mathbf{a}}_{n-1}\,\Delta t^2$. The particle displacement responses to an acceleration are

$$X/A\,\Delta t^2 = c_0 + c_1/z + c_2/z^2 + \cdots + z/(z-1)^2 \tag{14a}$$

and

$$X/A\,\Delta t^2 = z^2(z-1)^{-2}(d_0 + d_1/z + d_2/z^2 + \cdots)^{-1}, \tag{14b}$$

where $(x_n, a_n) = (X, A)\,z^n$, $z = \exp(-i\omega\,\Delta t)$, $d_0 + d_1 + d_2 + \cdots = 1$ for D schemes in general, and $d_0 = 2$ and $d_1 = -1$ for the D_1 scheme.

We next employ the methods of [9] and [10] to analyze the effects of strict spatial differencing. Specializing to the class of momentum conserving schemes, from [2] we have for the implicit increment to the charge density $\delta\rho$ and the polarization P,

$$\delta\rho_j = -\frac{P_{j+1/2} - P_{j-1/2}}{\Delta x}, \qquad P_{j\pm 1/2} = \sum_{j'} \chi_{j\pm 1/2, j'}\,\delta E_{j'},$$

where

$$\chi_{j\pm 1/2, j'} = \beta\,\Delta t^2 \sum_i \frac{q_i^2\,\Delta x}{m_i}\,S_m(X_{j'} - x_i)\,S_{m-1}(X_{j+1/2} - x_i)$$

from Eq. (70) of [2]. The particle interpolation functions satisfy the identity

$$\frac{d}{dx}S_m = \frac{1}{\Delta x}\,[S_{m-1}(x + \Delta x/2) - S_{m-1}(x - \Delta x/2)],$$

which is Eq. (50) of [2]. We Fourier transform the equations in space and obtain

$$\delta\rho(k) = -\beta\omega_p^2 \Delta t^2 \sum_p \kappa(k_p)\, k_p S_m^2(k_p)\, \phi(k),$$

while for the explicit contribution to the charge density we have

$$\rho(k) = -\omega_p^2 \Delta t^2 (X/A\, \Delta t^2 - \beta) \sum_p \kappa(k_p)\, k_p\, S_m^2(k_p)\, \phi(k).$$

The explicit contribution to the charge density was obtained by subtracting the implicit increment to the particle displacement response from the total response $X/A\, \Delta t^2 - \beta$. The modifications in $\rho(k)$ due to the spatial grid were derived in [9] and [10]. Finally, from Poisson's equation $-\nabla^2\phi = \rho + \delta\rho$ we obtain the cold-plasma dispersion relation

$$\varepsilon = 1 + (X/A\, \Delta t^2)\, \omega_p^2 \Delta t^2 K^{-2} \sum_p k_p \kappa(k_p)\, S_m^2(k_p) = 0, \tag{15}$$

where $k_p = k - pk_g$, $k_g = 2\pi/\Delta x$, and $-K^2$, $i\kappa(k_p)$, and $S_m(k_p)$ are the Fourier transforms of the difference representations d^2/dx^2, d/dx and the mth order particle spline, e.g., $S_m(k) = [\sin(k\, \Delta x/2)/(k\, \Delta x/2)]^{m+1}$. This result was anticipated from the analysis of [9].

The solutions of Eq. (15) are identical to those described in [3] with no grid effects if we replace $\omega_p^2 \Delta t^2$ with $\omega_p^2 \Delta t^2 K^{-2} \sum k_p \kappa(k_p)\, S_m^2(k_p)$ in the earlier analysis. In other words, the solutions of the C and D scheme dispersion relations described in [3] exactly correspond to the solutions of Eq. (15) here, if we include the $k\, \Delta x$-dependent correction factors in the definition of $\omega_p^2 \Delta t^2$ (see Fig. 1, for example). For finite $\omega_p^2 \Delta t^2$, the grid introduces $k\, \Delta x$ corrections to the dispersion relations in the usual way [10]; grid effects are especially pronounced as k approaches $\pi/\Delta x$. For $k\, \Delta x \neq \pi$ and $\omega_p^2 \Delta t^2 \to \infty$, grid effects are negligible.

For sake of definiteness and to correspond to simulation examples described here subsequently, Eq. (15) has been specialized to momentum conserving schemes. We have also analyzed the linear dispersion relation for simple harmonic oscillations in a Hamiltonian algorithm with a direct implicit field solution [2]. This analysis recovers the result of Appendix B in [11]; there are *no* grid modifications to the cold plasma dispersion relation in the Hamiltonian algorithm,

$$\varepsilon = 1 + (X/A\, \Delta t^2)\, \omega_p^2 \Delta t^2 = 0. \tag{16}$$

[As in the case of explicit formulations, energy is *not* necessarily conserved by the implicit version of the Hamiltonian method for finite Δt.]

When inconsistent spatial smoothing or ad hoc spatial differencing is introduced, Eq. (15) is altered. In particular, if $-\nabla \cdot [\chi^{(r)} \nabla\, \delta\phi^{(r+1)}]$ in Eq. (5) is inconsistently smoothed or its differencing simplified, the modified dispersion relations are

$$\varepsilon = \beta\omega_p^2 \Delta t^2 K^{-2} (\tilde{S}_k - \tilde{S}'_k) \sum_p k_p\, \kappa(k_p)\, S_m^2(k_p), \tag{17}$$

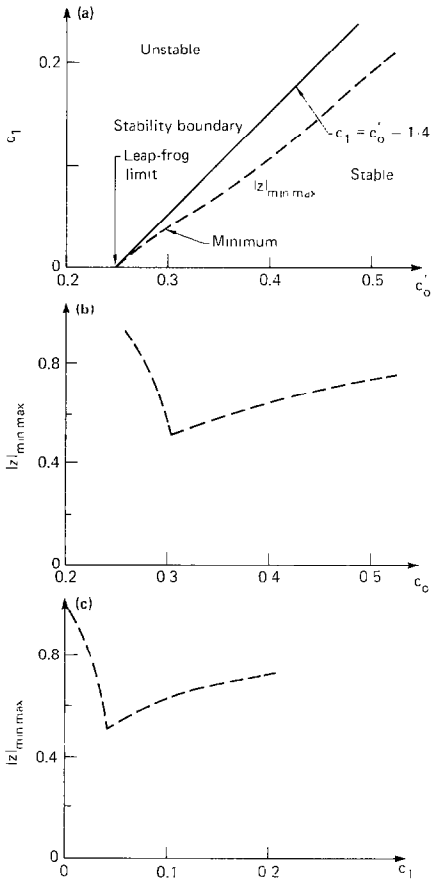

FIG. 1. (a) Stability diagram for difference schemes with $c_0, c_1 \neq 0$ and $c_{s\geqslant 2} \equiv 0$, $c_0' \equiv c_0 + 1/\omega_p^2 \Delta t^2$ from [3]. The values of c_0, c_1, and $\omega_p^2 \Delta t^2$ are redefined to include the modifications due to spatial differencing and smoothing, e.g., see Eqs. (15) and (17), or the shifts due to extrapolation, as in Eqs. (20) and (26). The locus of points, along which the maximum value of $|z|$ is minimized, is labeled $|z|_{\min-\max}$. The absolute minimum $|z|$ of the most weakly damped normal mode occurs at $c_0 \cong 0.3$, $c_1 \cong 0.04$ and $|z| \cong 0.5$. (b) The $|z|_{\min-\max}$ curve minimized with respect to c_1 plotted against c_0'. (c) The $|z|_{\min-\max}$ curve minimized with respect to c_0' plotted against c_1.

where ε is given in Eq. (15), with $\omega_p^2 \Delta t^2 \to \tilde{S}_k \omega_p^2 \Delta t^2$, $\beta = c_0$ or d_0^{-1} for the C or D schemes, and $(\tilde{S}_k - \tilde{S}_k')$ is the Fourier transform of the consistent smoothing operator minus the inconsistent smoothing operator and/or correction for simplified differencing.

We observe in Eqs. (12), (13), and (17) a similarity in the forms of the deviation from exact convergence and the shifts of the dispersion relation. All are proportional to the differences of smoothing or difference operators weighted by $\beta\omega_p^2 \Delta t^2$.

An example of the influence of spatial differencing on linear dispersion and the

changes produced by simplified differencing [2] is given as follows. For linear weighting, $S_1 = [\sin(k_p \Delta x/2)/(k_p \Delta x/2)]^2$. Birdsall and Langdon [10] show that

$$K^{-2} \sum_p k_p \kappa(k_p)\, S_1(k_p) = \cos^2(k \Delta x/2),$$

where $\kappa(k_p) = k_p \sin(k_p \Delta x)/(k_p \Delta x)$ and $K^2 = k^2[\sin(k \Delta x/2k \Delta x/2)]^2$ for two-cell and three-cell centered first and second difference operators. As described in [2], the Fourier transform of the strictly differenced $-\nabla \cdot \chi \nabla \delta\phi$ contains $\sin^2(k \Delta x)/\Delta x^2$ because of the product of the centered two-cell difference operators, in contrast to the corresponding $K^2 = k^2[\sin(k \Delta x/2)/(k \Delta x/2)]^2$ that arises in simplified differencing. Hence, $\tilde{S}_k/\tilde{S}'_k = [(\sin k \Delta x)/2 \sin(k \Delta x/2)]^2 = \cos^2(k \Delta x/2)$, where $\tilde{S}_k$ and $\tilde{S}'_k$ were introduced in Eq. (17); and the linear dispersion relations for a cold non-drifting plasma are

$$1 + (X/A\, \Delta t^2)\, \omega_p^2 \Delta t^2 \cos^2(k \Delta x/2) = 0 \tag{18a}$$

for strict differencing and

$$1 + (X/A\, \Delta t^2 - \beta)\, \omega_p^2 \Delta t^2 \cos^2(k \Delta x/2) + \beta \omega_p^2 \Delta t^2 = 0 \tag{18b}$$

for simplified differencing. Equations (14a) and (14b) give $X/A\, \Delta t^2$ for C and D schemes.

For strict dfferencing the solutions of Eq. (18a) correspond to those described earlier in [3] if the factor $\cos^2(k \Delta x/2)$ is absorbed into the effective value of $\omega_p^2 \Delta t^2$ as indicated in our discussion of Eq. (15). The dispersion relation for C schemes with simplified differencing becomes

$$1 + [c_0/\cos^2(k \Delta x/2) + c_1/z + c_2/z^2 \cdots + z/(z-1)^2] \times \omega_p^2 \Delta t^2 \cos^2(k \Delta x/2) = 0. \tag{19}$$

To use the solutions already obtained in [3], we define an effective value of $\omega_p^2 \Delta t^2$ as $\omega_p^2 \Delta t^2 \cos^2(k \Delta x/2)$ and an effective c_0 as $c_0/\cos^2(k \Delta x/2)$. Because $\cos^2(k \Delta x/2) \leqslant 1$, the effective value of $\omega_p^2 \Delta t^2$ is reduced and the effective value of c_0 is increased. For $\omega_p^2 \Delta t^2 \cos^2(k \Delta x/2) \ll 1$, the shift in the real part of the plasma frequency is $[\omega_p \Delta t \cos(k \Delta x/2)]^2[1/12 - c_0/\cos^2(k \Delta x/2) - c_1 - \cdots]/2$ and the damping rate is decreased by grid effects, $\mathrm{Im}(\omega/\omega_p) = [\omega_p \Delta t \cos(k \Delta x/2)]^3(c_1 + 2c_2 + \cdots)/2$. Because of the spatial differencing, the effective value of c'_0 in Fig. 1 is $c'_0 \equiv (c_0 + 1/\omega_p^2 \Delta t^2)/\cos^2(k \Delta x/2)$ with simplified differencing, which increases monotonically with increasing $k \Delta x < \pi$. The value of c_1 is unaffected, and the operating point of the C_1 scheme moves to the right in Figs. 1a and 1b. If the values of c_0 and c_1 correspond to those in the optimized C_1 scheme [3], where z is a minimum in Fig. 1, the effect of finite $k \Delta x$ is to shift z to larger values because of the increase in the effective c'_0. This indicates a decrease in the damping when simplified differencing is used. Spatial smoothing of the shortest wavelength modes would be beneficial here.

For $\omega_p^2 \Delta t^2 \to \infty$ and all wavelengths such that $\cos^2(k\Delta x/2) = 0$, the optimized C_1 scheme with strict differencing remains at the c_0, c_1 operating point that maximizes damping.

A specific illustration of the changes in linear dispersion caused by spatial differencing is given in Table I. We have used Eqs. (15), (17)–(19) to analyze results from the one-dimensional DIMPLES [6] code for a centered implicit integration scheme ($c_0 = 1/4$, $c_{s\geqslant 1} = 0$). Table I gives a comparison of code results for a cold plasma oscillation with solutions of Eqs. (18) and (19) for $\omega_p \Delta t = 10$ and linear weighting. Tabulated is $\tau \equiv 2\pi/\delta\omega$, where $\delta\omega = \pi/\Delta t - \omega$. The period τ was measured directly in the simulation as twice the time interval separating successive minima in the electric field energy density of a particular Fourier mode. The results from DIMPLES are well described by the linear dispersion theory for both strict and simplified differencing.

4.2. *Influence of Electric-Field Extrapolation*

In an earlier paper [2] and in Section 3, we described how implicit solution of the field and particle equations attempts to reduce the error in the approximate solution of the field equation to zero. As shown in our calculations of convergence here and in [2], if spatial smoothing is consistent and strict differencing is used, then errors that are linear in δx vanish identically. However, the coupled field and particle equations are nonlinear. Errors that are nonlinear in δx emerge in the implicit charge density calculated in any method based on linearization; this includes both the direct and moment methods. Here we address extrapolation methods that reduce nonlinear errors and assess what changes in linear dispersion characteristics result.

One of the more obvious sources of errors in implicit algorithms arises from particles that cross cell boundaries. In the scheme outlined in Eqs. (2)–(4), linearization is made around particle positions $\tilde{x}_{n+1}$. However, the increment to $\tilde{x}_{n+1}$ given by $\beta \Delta t^2 a_{n+1}$ may cause cell crossings and hence nonlinear errors in ρ_{n+1} that clearly are omitted in Eq. (2).

Linearization made around a better estimate of x_{n+1}, an $x_{n+1}^{(0)}$ that is an extrapolation including electric-field effects, should better resolve field variations and reduce nonlinear errors in the implicit prediction of ρ_{n+1}. This could result in better accuracy for the same number of corrector iterations, especially for no corrector

TABLE I

Cold Plasma Oscillation Period for $\omega_p \Delta t = 10$

	Strict Differencing		Simplified Differencing [2]	
$k\Delta x$	τ	τ_{theory}	τ	τ_{theory}
$\pi/16$	157.9	158.3	142.9	142.1
$\pi/8$	156.7	156.2	113.2	113.1

iterations, or reduce the required number of iterations. Actually achieving these improvements with clever extrapolation depends on whether stability and desirable linear dispersion properties are compromised and may require deposition of additional particle data on the mesh.

Consider the iterative form of Poisson's equation given by Eq. (5). We allow for the possible use of the old electric field E_n as a first estimate of the advanced electric field, $E_{n+1}^{(0)} = E_n$. We also include inconsistent spatial smoothing or ad hoc spatial differencing represented by the operator $\tilde{S}'$. Poisson's equation becomes

$$-\nabla \cdot [1 + \tilde{S}'\chi] \nabla \delta\phi_{n+1} = \rho_{n+1}^{(0)} + \nabla^2 \phi_{n+1}^{(0)}, \tag{20}$$

where $\chi = \beta\omega_p^2(x_{n+1}^{(0)})\,\Delta t^2$, $\phi_{n+1} = \delta\phi_{n+1} + \phi_{n+1}^{(0)}$, $\phi_{n+1}^{(0)} = \theta\phi_n$, and $\theta = 0$ or 1. For class C schemes, the particle equations are

$$x_{n+1}^{(0)} = x_n + v_{n+1/2}\,\Delta t + c_0(\theta - 1)\,a_n\,\Delta t^2 + c_1(a_n - a_{n-1})\,\Delta t^2 + \cdots \tag{21a}$$

$$v_{n+1/2} = v_{n-1/2} + a_n\,\Delta t \tag{21b}$$

$$x_{n+1} = x_{n+1}^{(0)} + c_0(a_{n+1} - \theta a_n)\,\Delta t^2 \tag{21c}$$

and $\beta = c_0$. This is an example of the predictor scheme described in Section 3.2 of [2].

We linearize these equations for the case of a cold, uniform plasma. Fourier transform in space, and absorb spatial-grid modification factors in the effective value of $\omega_p^2\,\Delta t^2$ [see Eqs. (15) and (17)]. With $z \equiv \exp(-i\omega\,\Delta t)$, we obtain a dispersion relation for a cold plasma

$$\begin{aligned} 1 + \tilde{S}_k\omega_p^2\,\Delta t^2[c_0 + c_1/z + c_2/z^2 + \cdots + z/(z-1)^2] \\ = (\tilde{S}_k - \tilde{S}_k')\,c_0\omega_p^2\,\Delta t^2(1 - \theta/z), \end{aligned} \tag{22}$$

where $\tilde{S}_k$ and $\tilde{S}_k'$ are the Fourier transforms containing the grid modification factors for strict differencing and consistent smoothing ($\tilde{S}_k$) and for ad hoc differencing and inconsistent smoothing ($\tilde{S}_k'$).

Part of the right side of Eq. (22) was obtained previously in Eq. (17). The new θ/z term in Eq. (22) creates a phase error originating from the use of the extrapolated electric field. This new term can be combined with the c_1/z term on the left side and leads to a new value for the effective c_1. Note, however, that the right side of Eq. (22) vanishes when $\tilde{S}_k = \tilde{S}_k'$, and the dispersion relation Eq. (15) is recovered. Thus, we see that with inconsistent smoothing or ad hoc differencing ($\tilde{S}_k - \tilde{S}_k' \neq 0$), the effective values of c_0 and c_1 are both changed. In normal circumstances, the shortest wavelength modes will be the most affected. Increasing c_0 improves stability, while increasing c_1 degrades stability and produces more damping in stable oscillations [3]. At small $\omega_p^2\,\Delta t^2$, c_0 and c_1 contribute additively in shifting the real part of the frequency [3]. If the combination of ad hoc differencing and extrapolation of the electric field ($\theta = 1$) leads to instability near the Nyquist frequency, increasing c_0 can

restore stability. With the appropriate re-definitions of c_0 and c_1, Fig. 1 displays many of these properties. Increased implicitness and dissipation were required to ensure good code performance when simplified differencing was employed in Mason's implementation of the implicit moment method [12]. Dissipation necessarily accompanied the implicitness because of the first-order-accurate temporal differencing used [3].

A similar analysis can be performed for D schemes. In place of Eq. (21) we have

$$x_{n+1}^{(0)} = x_n + v_{n+1/2}^{(0)} \Delta t \tag{23a}$$

$$v_{n+1/2}^{(0)} = v_{n-1/2} + \frac{\theta a_n}{d_0} \Delta t - \frac{d_1}{d_0}(v_{n-1/2} - v_{n-3/2}) - \frac{d_2}{d_0}(v_{n-3/2} - v_{n-5/2}) - \cdots \tag{23b}$$

$$x_{n+1} = x_n + v_{n+1/2} \Delta t \tag{23c}$$

$$v_{n+1/2} = v_{n-1/2} + a_{n+1} \frac{\Delta t}{d_0} - \frac{d_1}{d_0}(v_{n-1/2} - v_{n-3/2}) - \frac{d_2}{d_0}(v_{n-3/2} - v_{n-5/2}) - \cdots. \tag{23d}$$

For D schemes $\beta = d_0^{-1}$. The resulting dispersion relation for a cold, uniform plasma is then

$$1 + S_k \omega_p^2 \Delta t^2 \frac{z^2}{(z-1)^2 D} = (S_k - S_k') \frac{\omega_p^2 \Delta t^2}{d_0} \left(1 - \frac{\theta}{z}\right), \tag{24}$$

where $D = d_0 + d_1/z + d_2/z^2 + \cdots$. As with C schemes, extrapolation of the electric field in conjunction with inconsistent smoothing or ad hoc differencing can introduce a phase shift in the dispersion relation in the form of the θ/z term.

Both extrapolation schemes suggested in the preceding can produce phase errors that alter the linear dispersion properties and the stability characteristics. In general, these modifications are largest where $|\tilde{S}_k - \tilde{S}_k'|$ is biggest, typically at very short wavelengths. However, an alternative extrapolation scheme that cannot shift the dispersion and linear stability characteristics might be more desirable.

The following class of extrapolation schemes does *not* introduce phase errors in the dielectric response. Consider a general method for extrapolating to $x_{n+1}^{(0)}$, and define $\tilde{x}_{n+1} = x_{n+1} - \beta a_{n+1} \Delta t^2$. If we subtract $x_{n+1}^{(0)}$ from x_{n+1}, we obtain

$$x_{n+1} - x_{n+1}^{(0)} = \beta a_{n+1} \Delta t^2 + \tilde{x}_{n+1} - x_{n+1}^{(0)}. \tag{25}$$

Forming the charge density ρ_{n+1} from a linear expansion of $\sum_i qS(X_j - x_{i,n+1})$ around $x_{n+1}^{(0)}$, we find

$$\rho_{n+1} = \rho_{n+1}^{(0)} - \sum_i qS'(X_j - x_{i,n+1}^{(0)})(\beta a_{i,n+1} \Delta t^2 + \tilde{x}_{i,n+1} - x_{i,n+1}^{(0)}). \tag{26}$$

The corresponding field equation is

$$-\nabla \cdot (1+\chi)\nabla\phi_{n+1} = \sum_i qS(X_j - x^{(0)}_{i,n+1}) - \sum_i qS'(X_j - x^{(0)}_{i,n+1}) \times (\tilde{x}_{i,n+1} - x^{(0)}_{i,n+1}), \tag{27}$$

where $\chi = \beta\omega_p^2 \Delta t^2$ is constructed from particle positions $\{x^{(0)}_{i,n+1}\}$. The right side of Eq. (27) requires deposition of two scalar quantities accumulated from the particle data, of which one is the charge density $\rho^{(0)}_{n+1}$.

The derivation of the linear dispersion relation for Eqs. (25) and (27) in the limit of a cold, uniform plasma is straightforward. Including the possibility that the susceptibility term on the left side of (27) is inconsistently smoothed or differenced in space, we obtain

$$1 + \tilde{S}_k \omega_p^2 \Delta t^2 X/(A\,\Delta t^2) = (\tilde{S}_k - \tilde{S}'_k)\beta\omega_p^2 \Delta t^2, \tag{28}$$

where $X/(A\,\Delta t^2)$ is given in Eqs. (14a) and (14b) for the C and D schemes and $\beta = c_0$ and d_0^{-1}, respectively. The definitions of $\tilde{S}_k$ and $\tilde{S}'_k$ are identical to those introduced in Eq. (22). This result is identical to Eq. (17); *no* phase-shift producing term has been introduced. Note also that the linear dispersion relation is independent of the specific choice of $x^{(0)}_{n+1}$. Although the right side of Eq. (27) is a representation of $\tilde{\rho}$, it is *not* the same as $\tilde{\rho}$, even for linear S, when $|\tilde{x}_i - x^{(0)}_{i,n+1}| > \Delta x$; and for nonlinear S, it is not equal to $\tilde{\rho}$ for any $|\tilde{x}_i - x^{(0)}_{i,n+1}|$. However, in the linear dispersion relation for cold plasma oscillations, the right side of Eq. (27) is the same as $\tilde{\rho}$ and $\chi(x^{(0)}_{i,n+1})$ can be set equal to $\chi(\tilde{x}_i)$.

5. Conclusion

Analysis and code experimentation indicate that inconsistent smoothing, ad hoc spatial differencing, and electric-field extrapolation can modify the convergence and linear-dispersion characteristics of all implicit simulation schemes. Inconsistent smoothing and simplified differencing can degrade convergence; the concomitant shift in the linear dispersion relations and the loss of convergence share a common mathematical structure. With adequate suppression of oscillations at $\omega \approx \pi/\Delta t$, electric-field extrapolation should improve nonlinear accuracy of the solution of the field and particle equations. Our analysis of two general schemes combining extrapolation with implicit field solution demonstrates that it is possible to avoid the introduction of phase errors and the associated degradation of stability.

In general, the changes in convergence and linear dispersion properties due to inconsistent smoothing, ad hoc spatial differencing, and extrapolation can be substantial, but difficulties can be circumvented. The most significant changes occur at short wavelengths where smoothing should help control unwanted effects. Furthermore, our analysis suggests how to alter parameters in the C and D schemes to compensate for any substantive degradation of stability and dispersion characteristics. Similarly, Denavit's analysis of linear dispersion including finite Δt and Δx

effects guides algorithm optimization and has helped in understanding simulation performance of the implicit moment method [13].

A number of important related issues have *not* been addressed here. For example, one wonders what influence simplified differencing has on artificial cooling and heating [3, 12]. By causing mild numerical instability, simplified differencing may be responsible for artificial plasma heating. On the other hand, if phase errors in the algorithm lead to numerical cooling as described in [3, 5], the cooling rate is proportional to $|\varepsilon(\mathbf{k}, \mathbf{k}\cdot\mathbf{v})|^{-2}\,\mathrm{Im}(X/A)$, where X/A is calculated in Eqs. (14a) and (14b) for C and D schemes; and the choice of simplified or strict spatial differencing then modifies the effects of the spatial grid and perhaps indirectly the cooling rate.

Code experience [1, 4, 6] with strict and simplified differencing has been encouraging; the direct method has proven reliable at very large time steps, e.g., $\omega_{pe}\Delta t = 10^3$ [4], and accurately reproduces low-frequency phenomena in one- and two-dimensional applications. The accuracy and convergence of algorithms without iteration through the particle and field equations on each time step are good. Analyses of convergence and linear dispersion continue to guide both algorithm design and code performance.

ACKNOWLEDGMENTS

We are grateful to D. Barnes, J. Brackbill, J. Denavit, D. Hewett, and R. Mason for their suggestions and encouragement. This work was performed under the auspices of the U.S. Department of Energy by the Lawrence Livermore National Laboratory under Contract W-7405-Eng-48.

REFERENCES

1. A. FRIEDMAN, A. B. LANGDON, AND B. I. COHEN, *Comm. Plasma Phys. Controlled Fusion* **6** (1981), 225.
2. A. B. LANGDON, B. I. COHEN, AND A. FRIEDMAN, *J. Comput. Phys.* **51** (1983), 107.
3. B. I. COHEN, A. B. LANGDON, AND A. FRIEDMAN, *J. Comput. Phys.* **46** (1982), 15.
4. D. C. BARNES AND T. KAMIMURA, Nagoya University Report IPPJ-570 (April, 1982); D. C. BARNES, T. KAMIMURA, J. N. LEBOEUF, AND T. TAJIMA, *J. Comput. Phys.* **52** (1983), 480.
5. A. B. LANGDON, Tenth Conference on Numerical Simulation of Plasmas, San Diego, 1983, 2A2 (Lawrence Livermore National Laboratory Report, UCRL-88979).
6. A. FRIEDMAN, B. I. COHEN, AND A. B. LANGDON, Tenth Conference on Numerical Simulation of Plasmas, San Diego, 1983, 2A3.
7. J. DENAVIT, Tenth Conference on Numerical Simulation of Plasmas, San Diego, 1983, 1B15.
8. C. R. MENYUK, "Some Properties of the Discrete Hamiltonian Method," University of Maryland Physics Publication No. 83–112 (Nov. 1982), *Phys. D*, in press.
9. A. B. LANGDON, *J. Comput. Phys.* **30** (1979), 202.
10. C. K. BIRDSALL AND A. B. LANGDON, "Plasma Physics Via Computer Simulation,," McGraw–Hill, New York, 1984.
11. A. B. LANGDON, *J. Comput. Phys.* **12** (1973), 247.
12. R. J. MASON, *J. Comput. Phys.* **41** (1981), 233.
13. J. DENAVIT, *J. Comput. Phys.* **42** (1981), 337.